Pharm Res (2015) 32:3213–3227
DOI 10.1007/s11095-015-1698-y

RESEARCH PAPER

Biomimicking Robust Hydrogel for the Mesenchymal Stem Cell Carrier

Byeongtaek Oh[1] • Russell B. Melchert[2] • Chi H. Lee[1,3]

Received: 27 February 2015 / Accepted: 14 April 2015 / Published online: 25 April 2015

ABSTRACT

Purpose This study was aimed to develop a hydrogel-nanofiber as an advanced carrier for adipose derived human mesenchymal stem cells (AD-MSCs) and evaluate its potential for immunomodulatory therapies applicable to surface coating of drug eluting stent (DES) against coronary artery diseases (CAD).

Methods A mixture of dispersing-nanofibers (dNFs) and poly (ethylene glycol)-diacrylate (PEGDA) were blended with sodium alginate to achieve robust mechanical strength. The effects of stem cell niche on cell viability and proliferation rates were evaluated using LDH assay and alamar blue assay, respectively. The amount of Nile-red microparticles (NR-MPs) remained in the hydrogel scaffolds was examined as an index for the physical strength of hydrogels. To evaluate the immunomodulatory activity of AD-MSCs as well as their influence by ROS, the level of L-Kynurenine was determined as tryptophan replacement compounds in parallel with IDO secreted from AD-MSCs using a colorimetric assay of L-amino acid.

Results Both SA-cys-PEG and SA-cys-dNF-PEG upon being coated on stents using electrophoretic deposition technique displayed superior mechanical properties against the perfused flow. d-NFs had a significant impact on the stability of SA-cys-dNF-PEG, as evidenced by the substantial amount of NR-MPs remained in them. An enhanced subcellular level of ROS by spheroidal cluster yielded the high concentrations of L-Kynurenine (1.67 ± 0.6 μM without H_2O_2, 5.2 ± 1.14 μM with 50 μM of H_2O_2 and 8.8 ± 0.51 μM with 100 μM of H_2O_2), supporting the IDO-mediated tryptophan replacement process.

Conclusion The "mud-and-straw" hydrogels are robust in mechanical property and can serve as an ideal niche for AD-MSCs with immunomodulatory effects.

KEY WORDS biomimicking hydrogel-nanofiber · coating of drug eluting stent · immunomodulatory effects · mesenchymal stem cells

ABBREVIATIONS

d-NFs	Dispersing-nanofibers
EPD	Electrophoretic deposition
IDO	Indoleamine 2,3-dioxygenase
NR-MPs	Nile-red microparticles
ROS	Reactive oxygen species
SA-cys	Hydrogel scaffolds made of Cysteine-conjugated sodium alginate
SA-cys-dNF	Hydrogel scaffolds made of SA-cys blended with dNFs
SA-cys-dNF-PEG	Hydrogel scaffolds made of SA-cys cross-linked with dNFs and PEG-DA
SA-cys-PEG	Hydrogel scaffolds made of SA-cys cross-linked with PEG-DA

INTRODUCTION

Coronary artery disease (CAD) is most commonly caused by atherosclerotic occlusion and generally results in myocardial infarction and angina (1). Despite advances in drug-eluting stent (DES) for angioplasty, DES has had limited ability to prevent restenosis and contributes to late-stage thrombosis (2). Subsequently, this complication necessitates by-pass or

✉ Chi H. Lee
leech@umkc.edu

[1] Division of Pharmaceutical Sciences, School of Pharmacy, University of Missouri-Kansas City, Kansas City, Missouri 64108, USA

[2] Division of Pharmacology and Toxicology, School of Pharmacy, University of Missouri-Kansas City, Kansas City, Missouri 64108, USA

[3] Division of Pharmaceutical Sciences, University of Missouri at Kansas City, 2464 Charlotte Street, HSB-4242, Kansas City, Missouri 64108, USA

further intervention. According to the recent reports, restenosis is mainly caused by the degradation of plaque that is accelerated by the secretion of inflammatory cytokines from mast cells (MCs) and the high level of reactive oxygen species (ROS) (3–5).

Regulation of the immune response has been widely explored for the development of advanced cardiovascular stents, yet progress thus far made in producing novel vascular stents to modulate the immunoresponse has not been significant. It was recently reported that MCs present in atheroma have played a critical role in the apoptosis process of human vascular endothelial cells (hECs). In our previous study, Nitric Oxide (NO) in a combination with the ROS scavenger, Edaravone, down-regulated the secretion of inflammatory cytokines (5), resulting in the enhancement of viability of hECs undergoing MC-mediated external stress.

Among various stem cells, mesenchymal stem cells (MSCs) are unique in that they have immunosuppressive and immunomodulatory activities, producing suppression of the proliferation rates of both innate and adaptive immune cells (6,7). MSCs activate regulatory T-cells (Tregs) through the mechanisms involved with direct cell-cell interaction and induction of various soluble factors, such as prostagladin E2, indoleamine 2,3-dioxygenase (IDO) and interleukin-6 (IL-6) (8–12). In addition, cytokines secreted by MSCs promoted *in vitro* and *in vivo* arteriogenesis (13) and subsequently affected therapeutic efficacy of MSCs (11). The availability and versatility of MSCs make them a novel immunological therapeutic tactic to prevent atherosclerotic occlusion (14–16).

The terms 'bio-similar', 'bio-mimetic' and 'bio-inspired' were introduced to delineate an alternative and efficient design of a cell-delivery carrier (17). It was previously proposed that sodium alginate would form a 3D cell-gel hydrogel on indium-tin-oxide (ITO)-glass via electrical-stimulation process (18). Moreover, the hydrogel composited with filamented-polylactic acid (PLA) nanofibers prepared from aminolysis-assisted fragmentation could be biologically active and stimulate cell-signaling pathways (19). Nanocomposite hydrogels inspired by the ordered "brick and mortar" arrangement were also fabricated using inorganic and organic layer modification (17). The resulting materials generally display unique combinations of strength and toughness, but have proven difficulty in synthetically mimicking the biological systems (20). Moreover, the feasibility of those formulations as a cell-delivery carrier has not been practically investigated.

The aim of this study was to develop and evaluate the biomimicking "mud-and-straw bird nest" as an advanced cell-delivery carrier for MSCs. A bio-inspired hydrogel-nanofiber for adipose derived human mesenchymal stem cells (AD-MSCs) was explored as an immunomodulatory carrier to be applicable to the surface coating of DES. A mixture of dispersing-nanofibers (dNFs) and poly (ethylene glycol)-diacrylate (PEGDA) was blended with sodium alginate which yields robust mechanical strength against the continuous perfused fluid and dynamic environment of the myocardium. The effects of stem cell niche made of a mixture of dNF and PEGDA on cell viability and proliferation rates were evaluated using LDH assay and alamar blue assay, respectively. The amount of Nile-red microparticles (NR-MPs) remained in the hydrogel scaffolds after being placed in a pseudo-perfusion chamber for 7 days was examined as an index for the physical strength of hydrogels. To evaluate the immunomodulatory activity of AD-MSCs as well as their influence by ROS, the level of $_{L}$-Kynurenine was determined as tryptophan replacement compounds with Indoleamine 2,3-Dioxygenase (IDO) secreted from AD-MSCs using a colorimetric assay of $_{L}$-amino acid.

METHODS AND MATERIALS

Materials

Poly (L-lactic acid) (PLA) was purchased from Polysceinces Inc. (Warrington, PA). Poly lactic-co-glycolic acid (PLGA) was purchased from Lakeshore Biomaterials (Birmingham, AL). Sodium alginate (SA), 5,5′-Dithiobis(2-nitrobenzoic acid) (DTNB), dichloromethane (DCM), Fluorescent sodium salt (FS), ethylenediaminetetraacetic acid (EDTA), 1-Ethyl-3-(3-dimethylaminopropyl) carbodiimide (EDC), cysteine hydrochloride monohydrate, Nile-red (NR), hexamethylenediamine (HDA), 2-isopropanol (IPA), 2-hydroxy-4′-(2-hydroxyethoxy)-2-methylpropiophenone (Irgacure 2959), trichloroacetic acid, 4-dimethylaminobenzaldehyde, $_{L}$-kynurenine, poly (ethylene glycol) diacrylate (PEGDA, Mn= 575) and ninhydrin were purchased from Sigma-Aldrich (St. Louis, MO). 1,1,1,3,3,3 Hexafluoro-2-propanol (HFIP) was purchased from CovaChem (CovaChem, LLC., IL). Tumor necrosis factor-α (TNF-α) was purchased from R&D system (Minneapolis, MN).

Adipose-derived human mesenchymal stem cells (AD-MSCs) (PCS-500-011), mesenchymal stem cell basal medium (PCS-500-030), MSCs growth kit (PCS-500-040), vascular cell basal medium (PCS-100-030) and endothelial growth kit–VEGF (PCS-100-041) were purchased from ATCC (Manassas, VA). All other reagents and solvents were of analytical grade.

Preparation of Various Hydrogel Scaffolds

Synthesis of Thiolated-Alginate (SA-cys)

Sodium alginate cysteine conjugates (SA-cys) were prepared by EDC technique (21). Briefly, 2% (w/v) of SA was dissolved overnight in distilled and deionized (DI) water. 200 mM EDC solution was added to the polymer solution and then

incubated for 1 h. After the incubation, 1% (w/v) of cysteine solution was added to the mixture, which was allowed for the reaction to proceed at room temperature overnight. To isolate SA-cys, the aqueous solution was dialyzed against 1 mM HCl for 2 days and subsequently 1% NaCl for 2 days. All preparations were conducted in the dark condition to minimize disulfide bond formation. Dialyzed samples were freeze-dried and kept at −20°C until further use.

Preparation of NR-Microparticles

NR-Microparticles (NR-MPs) were formulated using O/W emulsification (22). For the oil phase, 6% (w/v) of PLGA was dissolved in DCM, whereas, for the water phase, 1% (w/v) of PVA was dissolved in DI water with continuous stirring until it reached a homogenous steady phase. The oil phase was transferred into the water phase (the O/W solution) and mixed using a homogenizer (Ultra-Turrax, IKA). The emulsion was continuously stirred to fully evaporate the organic solvent. NR-Microparticles were collected from supernatant after ultracentrifugation (x 8,000 rpm for 30 min). The pellets containing microparticles were lyophilized and kept at −20°C until further usage.

Preparation of Dispersing Chitosan-g-Nanofibers (d-NFs)

PLA nanofibers were formulated through electrospinning technique (23). Dispersing-nanofibers (d-NFs) were prepared using a previously reported method after minor modification (19). Briefly, segmented-PLA nanofibers (1 cm^2) were incubated in IPA containing 8% (w/w) of HDA for 2 h. Aminolyzed-nanofiber meshes were gently washed with EtOH twice and then incubated in ethanol at 4°C for 24 h. After incubation, sliced nanofiber meshes were acquired using probe sonication (UltraSonic Probe 100, Fisher Scientific, Waltham, MA) (15 W for 30 s and pause for 5 s). d-NFs were collected from supernatant after ultracentrifugation (x 20,000 rpm for 30 min).

Segmented nanofibers were functionalized with chitosan using the two-step procedure (24). First, aminolyzed-dNFs were mixed with 2.5% (w/v) of glutaldehyde solution for 3 h. After the completion of mixing, the dNFs were filtered (0.22 μm) and incubated with 1% (w/v) chitosan solution at 4°C for 24 h. Chitosan-grafted dNFs acquired by ultracentrifugation (x 20,000 rpm for 30 min) were gently washed with DI water. The samples were lyophilized and kept at −20°C until further use.

Preparation of SA-cys Hydrogel Solution

The culture media was added with a mixture of 1% (w/v) of SA-cys, 0.4% (w/v) of d-NFs and 0.05% (w/v) of photoinitiator (Irgacure 2959, Sigma, St. Louis, MO) and steadily stirred until it reached a homogenous steady phase. The mixture was loaded with PEGDA (10% (v/v)) and labeled as SA-cys-dNF-PEG. For other solutions, SA-cys-PEG was prepared without d-NFs, whereas SA-cys was prepared in the absence of both d-NFs and PEGDA.

Characterization of Hydrogel Scaffolds

Swelling Ratio

The swelling ratios of the formulations were determined by measuring the water uptake content. The hydrogel-coated stents were immersed in 1 ml of PBS. The weights of the swelled hydrogel before and after being fully dried were determined. The swelling ratios at specific time intervals (5, 10, 15, 30, 45 and 60 min) were calculated using the following equations.

$$\textit{The Swelling Ratio}\,(\%) = [(S_w - S_d)/S_d] \times 100$$

where S_w is the weight of polymers with the absorbed water, and S_d is the weight of polymers free of residual moisture

Determination of Amine Groups (−NH_2) in hydrogel scaffolds

The derivatization process with ninhydrin, a chemical used to detect ammonia or primary and secondary amines, was used to determine the amount of -NH_2 groups grafted on the surface of d-NFs (25). Briefly, cardiovascular stent coated with hydrogel scaffolds were immersed in 1 M nynhydrin solution (40 μl) whose containers were placed into the water bath at 80°C and allowed for the reaction between ninhydrin and amine groups. After 15 min incubation, IPA (1 ml) was added to the solution for stabilization of the product. The concentrations in the solution were determined by measuring spectrophotometric absorbance at 540 nm (Spetronic 20D, Thermo Scientific, Waltham, MA). A calibration curve was produced with the standard samples of chitosan.

Determination of Thiol Groups (−SH) in hydrogel scaffolds

The thiol contents in hydrogel scaffolds upon being reacted with PEGDA via Michael-type addition was determined based on the color changes developed from the Ellman reagent detection process (21). Briefly, the solution of Ellman's reagent was prepared by dissolving 0.4% (w/v) of DTNB in 0.1 M sodium phosphate buffer (pH=8.0) containing 1 mM EDTA. Hydrogel-coated stents were immersed in 1 ml of sodium phosphate buffer containing 5 μl of Ellman's reagent, and incubated at room temperature for 15 min. Thiol contents were spectrophotometrically determined by measuring the optical absorbance at 441 nm. A calibration curve was

produced with a standard sample of cysteine hydrochloride monohydrate. For comparison purpose, both amine and thiol group in the samples produced via simple dip-coating method (i.e., used as the control groups) were also analyzed using the same procedure as described above.

In vitro Stability of Hydrogel Scaffolds against Shear Stress

A microfluidic perfusion chamber was designed for the stability test of hydrogel scaffolds under various conditions of variables and perfused flow rates (Mini-pump variable flow, Fisher Scientific, Waltham, MA). Cardiovascular stents coated with tested hydrogel scaffolds containing NR-microparticles were placed in the middle of tygon tubes, which were filled with test media (PBS with 2% of fetal-bovine serum (FBS)). The flow rate of the test media was intermittently increased up to 1 ml/s. The test media was replaced with the fresh media at specific time intervals and the amount of NR-MPs in the samples were quantified (5 min, 30 min, 1 h, 3 h, 6 h and 10 h for short-term analysis and 1, 2, 3, 5, and 7 days for long-term analysis).

To determine the amount of NR-MPs, the solutions containing NR-microparticles were spiked with acetone and sonicated to degrade the microparticles. The solution was vacuum-dried to evaporate acetone and then the NR concentration was determined using the multimode detector at excitation λ of 540 nm and emission λ of 640 nm (DTX 880, Beckman Coulter, Indianapolis, IN).

The shear stress imposed on cardiovascular stent was calculated by implementing such parameters as inner radius of tube ($a = 0.75 \times 10^{-3}$ m), viscosity ($\mu = 0.00098$ Pa-s) and flow rate ($Q = 1$ ml/s) to Poiseuille's law (26). For the stability test of the hydrogel scaffolds against the flow rate, the microfluidic chamber was placed under fluorescent microscopy (Leica DMI 3000D, Buffalo Grove, IL) with the intensities of FS (Fluorescent sodium salt) (excitation: 460 nm, emission: 520 nm). The percentage loss of NR-MPs were determined at specific time intervals (initial, 5 min, 30 min and 1 h) and used as an index of physical stability against the perfused flow in the vessel.

Stent Coating with AD-MSCs using Electrophoretic Deposition (EPD) Technique

When AD-MSCs were confluent, the cells were trypsinized, collected and centrifuged. The pellet was then mixed with the stock solutions (i.e. SA-cys, SA-cys-PEG, and SA-cys-dNF-PEG). The final concentration of AD-MSCs in the solution was adjusted to 2×10^6 cells/ml. The surface of cardiovascular stent was coated with the hydrogel using EPD technique under the applied voltage (1.5 V/cm^2) and a distance (0.5 cm) between anode and cathode for 30 s. The cell/hydrogel scaffolds coated on the stents were photopolymerized for 5 min under UV light with the intensity of 230 μW/cm^2 (Handheld UV lamp, Cole-Parmer, Vernon Hills, IL). After polymerization, the stents were placed in the vascular basal media containing VEGF (5 ng/ml) and incubated under the standard culture conditions (37°C and 5% CO_2).

For visual assessment of stability of stents coated with hydrogel scaffolds containing AD-MSCs, 0.1% (w/v) of fluorescein sodium salts (FS) was added in AD-MSCs, and the images of the fluorescent signals were examined using a microscope (Leica DMI 3000D, Buffalo Grove, IL).

Cell Culture Studies on Hydrogel Scaffolds

Viability of AD-MSCs loaded in Hydrogel Scaffolds

To evaluate the potential cytotoxicity of hydrogels loaded with AD-MSCs, homogeneous membrane integrity was analyzed by assessing LDH released into the media as a marker of dead cells.

Briefly, AD-MSCs (1×10^4 cells/well) were seeded on 96-well plate and then incubated overnight to allow the cells to attach to the bottom of the plate. For the cytotoxicity assessment of individual components of test formulations, such as SA-cys and d-NFs, the media was replaced with the fresh media having various concentrations of test formulations (SA-cys: 0, 0.25, 0.5, 1, and 2 mg/ml; d-NFs: 0, 0.2, 0.4, 0.6, and 0.8 mg/ml). The plate was incubated for 48 h and the media from each study was subjected to the LDH analysis (Promega, Madison, WI). For the positive control, the cells were lysed with 1% of Triton X-100 and the expression of LDH was measured using the same procedure as described above.

The potential cytotoxicity of hydrogels on AD-MSCs was evaluated using the live/dead staining kit (Calcein-AM for live cell staining and Ethidium homodimer for dead cell staining) (Abcam, Cambridge UK), and fluorescent images were recorded in a randomized and blind manner using a microscope (Leica DMI 3000D, Buffalo Grove, IL).

Assessment of the Proliferation Rate of AD-MSCs

The proliferation rates of AD-MSCs encapsulated in hydrogel scaffolds were quantified using Alamar Blue reagent (Life technologies, Grand Island, NY). Briefly, the cardiovascular stents coated with hydrogel scaffolds containing AD-MSCs (SA-cys, SA-cys-PEG and SA-cys-dNF-PEG) were incubated in 24-well plate with 9% of the Alamar Blue solution (2 ml). The plate was further incubated for 4 h to allow for viable cells to react with the reagent. Medium (20 μl) from the wells was transferred into 96-well plate to which 80 μl each of PBS was additionally added.

The proliferation rates were determined at specific time intervals (1,4,7,11) based on the fluorescent intensity of the solution (100 μl) measured using the multimode detector (excitation: 540 nm and emission: 590 nm). The relative fluorescent intensities were calculated with respect to those recorded at day 1.

Assessment of Immunomodulatory Activity of MSC

AD-MSCs have been highly effective in ameliorating implant rejection (27,28) and their immunomodulatory activity was known to be mediated by indolemaine 2,3-dioxygenase (IDO) (28). L-kynurenine is a tryptophan metabolite and known to contribute to the maintenance of a relative immune activity in MSC (29). It was also found that IDO and associated tryptophan/kynurenine transporter exchange mechanism were upregulated by such inflammatory inducers as cytokines, TNF-α and PGE_2 (30,31). To evaluate immunomodulatory activity of MSC, the level of L-kynurenine in AD-MSCs was determined as a depleting substance in parallel with IDO using a colorimetric assay of L-amino acid (32).

In brief, AD-MSCs seeded on 96-well plate (2×10^4 cells/well) were incubated with hydrogen peroxide (0, 50 and 100 μM) along with TNF-α (10 ng/ml) for 12 h. After incubation, the collected media were mixed with 30% of trichloroacetic acid at a ratio of 3:1 and incubated for 30 min at 50°C. They were centrifuged at 13,000 rpm for 3 min. The supernatants (100 μl) were diluted with 100 μl of Ehrlich reagent (2% (w/v) of 4-dimethylaminobenzaldehyde in glacial acetic acid) in a 96-well plate. The fluorescence absorbance was determined using a multimode detector at 490 nm and converted to the amount of IDO. A series of standard samples of L-Kynurenine were used to generate a calibration curve.

Effects of the ROS Level on Immunomodulatory Activity of MSC

The effects of ROS as an inflammatory inducer of the exchange process between IDO and associated tryptophan/kynurenine transporter on immune activity of MSC were also evaluated. The intracellular ROS level was analyzed using ROS sensitive dye (2′,7′–dichlorofluorescin diacetate, DCFDA) as previously reported (23). Briefly, after the cell matrix being disrupted by trypsinization, floated AD-MSCs were stained with 20 μM of DCFDA solution for 30 min at 37°C. Stained cells were washed with PBS twice and then supernatant was collected by centrifugation. The cells were suspended in the warm media for encapsulation. EPD technique was used for surface coating of stent with either SA-cys-PEG or SA-cys-dNF-PEG, and the hydrogel scaffold constructs were carefully detached from the metal surface using a surgical blade. The separated pieces of hydrogel were mounted on glass slides and five locations of each sample were visualized using fluorescent microscopy (Leica DMI 3000D, Buffalo Grove, IL) (excitation: 495 nm and emission: 529 nm). The fluorescent intensities of stained cells were analyzed using ImageJ (NIH, Bethesda, MD).

Statistical Analysis

Data were presented as a mean ± standard deviation (SD). One-way ANOVA was used to compare the means of independent samples. F-ratio was determined using SPSS software (SPSS, Chicago, IL) and Tukey's HSD was used for a post-hoc analysis. P values of less than 0.05 were considered as statistically significant. All experiments were conducted in triplicate unless otherwise specified.

RESULTS AND DISCUSSION

Preparation of Hydrogel Scaffolds

The hydrogel (mud)–nanofiber (straw) structure inspired by "mud-and-straw birds nest" was developed as an advanced cell-delivering carrier for AD-MSCs. PEGDA was used as a potent UV-assisted cross-linker between thiolated alginate and chitosan-functionalized dispersing nanofibers (d-NFs) (Figs. 1 and 2). The custom-built chamber was designed (Fig. 3) for EPD technique by which the stent surface was coated with the robust hydrogels (33). Upon being functionalized with cysteine in alginate chain (i.e., cysteine-conjugated sodium alginate), SA-cys yielded both an EPD interaction site and a thiol functional group that together constitute a robust mud-and-straw structure. As shown in Fig. 4, the cell-delivering capabilities of SA-cys produced a smooth surface layer coated on the surface of the stainless steel metal stent. In addition, the weights of polymer layers deposited on the stents through EPD technique were measured (SA-cys: 1.5 ± 0.1 mg/stent, SA-cys-dNF: 1.4 ± 0.3 mg/stent, SA-cys-PEG: 1.6 ± 0.3 mg/stent and SA-cys-dNF-PEG: 1.56 ± 0.25 mg/stent). The hydrogel scaffolds containing PEG showed an increase in the weights of polymer layer, but was not statistically significant, as compared to the scaffolds fabricated with either SA-cys or SA-cys-dNF.

Characterization of the Biomimetic Architecture of Hydrogel Scaffolds

The porous three-dimensional architecture of hydrogel scaffolds were examined using scanning electron microscopy (ESEM, XL 30, Hillsboro, OR). The micropore size of hydrogel scaffolds made of a mixture of PEG and d-NFs became smaller than those of SA-cys or SA-cys-PEG. PEG blending generally have a high impact on the morphological properties including a micropore size, whereas d-NFs not only affected

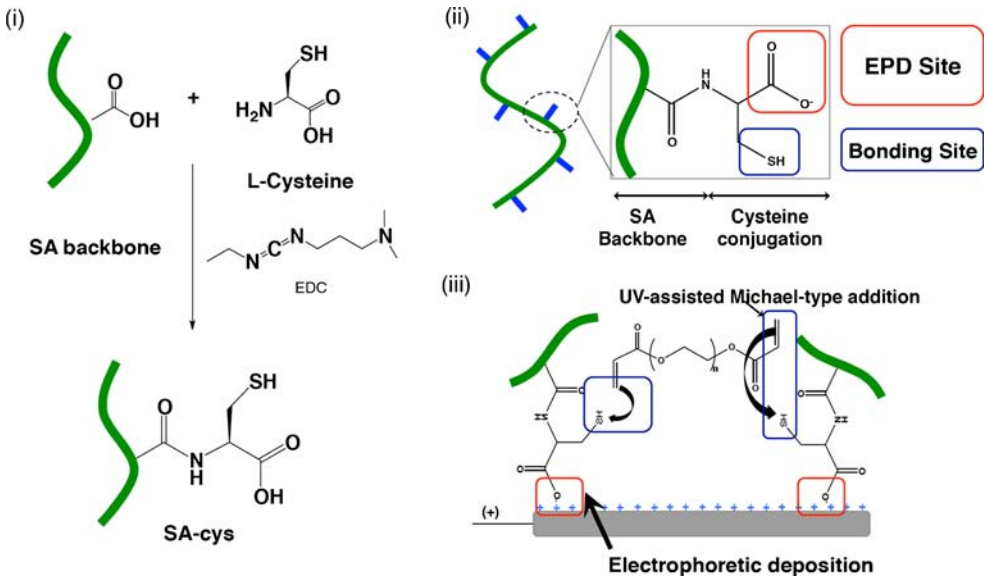

Fig. 1 (*i*) Graphical representation of the synthesis process of SA-cys. *Green* represents SA backbone. (*ii*) SA-cys has both a EPD available site and a crosslinkning site after cysteine conjugation. (*iii*) SA-cys deposition via EPD technique on the metalic surface with UV-assisted crosslinking. *Red and blue boxes* indicate EPD binding and crosslinking sites.

the morphological properties but also produced a smooth surface layer with tight junctions as represented by white arrows in Fig. 5.

EPD technique enhanced the quantity of red fluorescent signal reflecting NR-MPs present in the scaffolds (Fig. 6a) as compared to those produced by the dip-coating (DC) method, indicating that EPD technique could provide the strong electrical conductivity by which the hydrogel was loaded with the substantial amount of NR-MPs.

Distribution of AD-MSCs in Hydrogel Scaffolds and Encapsulation Efficacy

To elucidate the mechanism behind enhanced coating efficacy, surface potential (zeta-potential) variation during the fabrication process was determined using a standard dynamic light scattering instrument (DLS, Malvern, UK). Because the bilayer membranes possessed negative potential on the surface (34), the changes in zeta-potential of chitosan-grafted d-NFs containing fluorescent dye loaded-MPs (NR-MPs) (Fig. 6b) were monitored as a fraction of incubation time. The positive potential of d-NFs containing NR-MPs significantly decreased within 5 s, fluctuated for 1 min, and then reached a plateau (2.13 ± 0.12), indicating that d-NFs would form the clusters with MSCs through the charge-charge interaction.

The effects of d-NFs on distribution of AD-MSCs in hydrogel scaffolds produced by EPD technique was examined by the fluorescence microscopy image with stained fluorescent dyes (Live/Dead Assay) (Fig. 6c). As only live cells can lyse the AM-ester and allow calcein to freely permeate into the cell, the green fluorescence signal is indicative of live cells. Two hydrogel formulations, SA-cys-PEG and SA-cys-dNF-

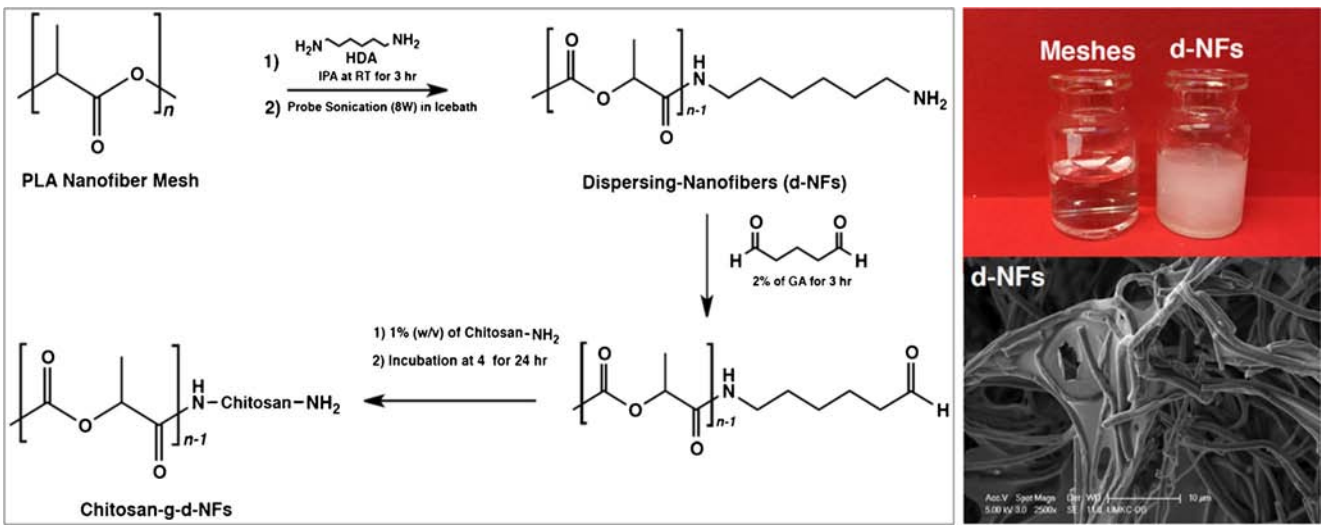

Fig. 2 Preparation of chitosan-grafted PLA nanofibers using the aminolysis-assisted fragmentation process.

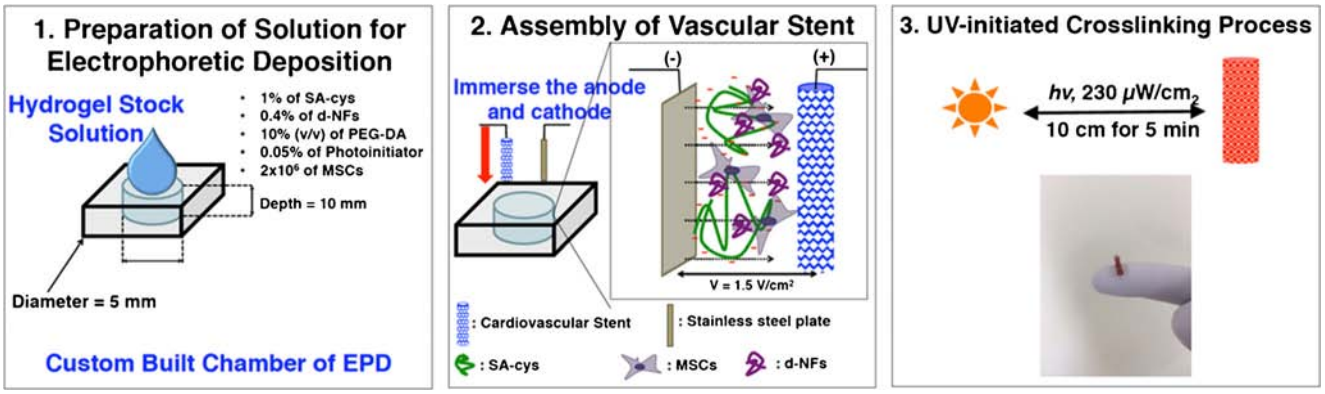

Fig. 3 1. Preparation of hydrogel stock solution for EPD technique. 2. Hydrogel deposition on cardiovascular stent using EPD technique performed in the custom-made chamber. 3. UV-assisted crosslinking process for the hydrogel construct.

PEG prepared by EPD technique, showed mostly green signals with the low level of red signals, indicating that they don't exert any adverse cytotoxicity.

The distribution profiles of AD-MSCs in hydrogel scaffolds were significantly influenced by the presence of d-NFs. For SA-cys-PEG, individual green signal was detected (Fig. 6c), whereas the signal produced high density clouds for the scaffolds made of d-NFs (SA-cys-dNF-PEG), indicating that AD-MSCs were substantially integrated with d-NFs. The results of this study support that SA-cys-dNF-PEG can serve as a proper stem-cell niche, overcoming the intrinsic limitations with hydrogels made of only alginate whose encapsulated cells are independently proliferating and growing without having to go through any cell-cell interactions.

Characterization of the Chemical Linkage in Hydrogel Scaffolds

The raman spectra were collected on inverted Raman confocal microscope (inVia Raman microscope, Renishaw; 20× objective (Leica DMI 3000D, IL) and a 785 nm (1.58 eV)).

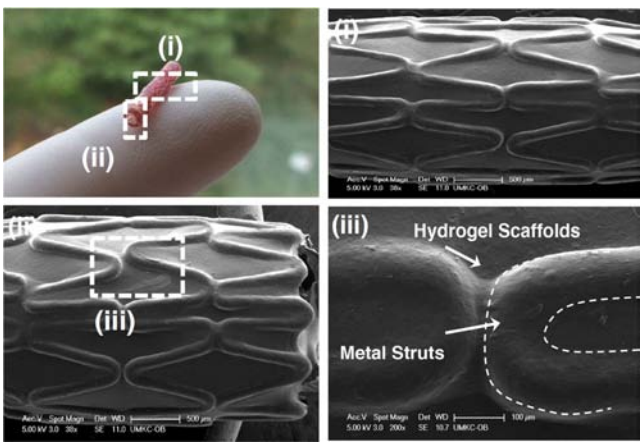

Fig. 4 Hydrogel-coated cardiovascular stent. (*i*) SEM image for the middle part of the stent; (*ii*) SEM image for the end part of the stent; and (*iii*) SEM images for metal strut with high magnification.

As shown in Fig. 7a, both SA and SA-cys had peaks representing a glycosidic ring breathing mode (1088–1098 cm^{-1}). The raman spectroscopy displayed unique peaks present in SA-cys (S-S stretching deformation near 457–510 cm^{-1}, −C-S- stretching near 727 cm^{-1}, −C=O stretching, N-H bend and C-N stretch near 1612–1637 cm^{-1}, S-H stretching near 2550–2590 cm^{-1}) (35). The SEM and microscopic fluorescent analyses successfully offered the demographic images of how chemical bonds (i.e. primary amine ($-NH_2$) from chitosan and thiol (−SH) from cysteine) interacted with di-acrylate bonds of PEGDA.

To investigate whether or not cysteine-functionalized SA made an additional bond with PEGDA, ninhydrin and ellman's assays were performed. The hydrogel scaffolds produced by DC had none or minimal $–NH_2$ density (Fig. 7b), whereas the hydrogel scaffolds produced by EPD technique had a greater amount of $–NH_2$ density (SA-cys-dNF: 78.7±5.2 and SA-cys-dNF-PEG: 47.2±4.0 μg/ml/stent), confirming d-NFs were deposited in the hydrogel scaffolds by EPD technique to a greater extent than those by DC method.

An addition of PEGDA reduced $–NH_2$ density in SA-cys-dNF-PEG as compared to SA-cys-dNF ($p<0.001$) mainly due to specific interactions of the acrylate group from PEGDA with primary amine in d-NFs, which formed a secondary amine. Because ninhydrin assay measures the amount of secondary amine, the quantity of primary amine in d-NFs (47.2±4.0 μg/ml/stent, $p<0.01$) reflects the Michael-type addition between primary amine and acrylate groups, which is in a close agreement with the previous report (36).

The concentration of -SH in various hydrogels was determined using Ellman's assay. As expected, SA-cys had a greater thiol content than SA (SA: 0.046±0.072 and SA-cys: 2.02±0.07 μg/ml/stent) (Fig. 7c), indicating that the amount of thiol group was significantly reduced when the hydrogel scaffolds containing PEGDA were exposed to UV (SA-cys-PEG: 1.9±0.2 and SA-cys-PEG with UV: 0.4±0.03 μg/ml/stent, $p<0.001$). For SA-cys-dNF-PEG, it had a similar reduction

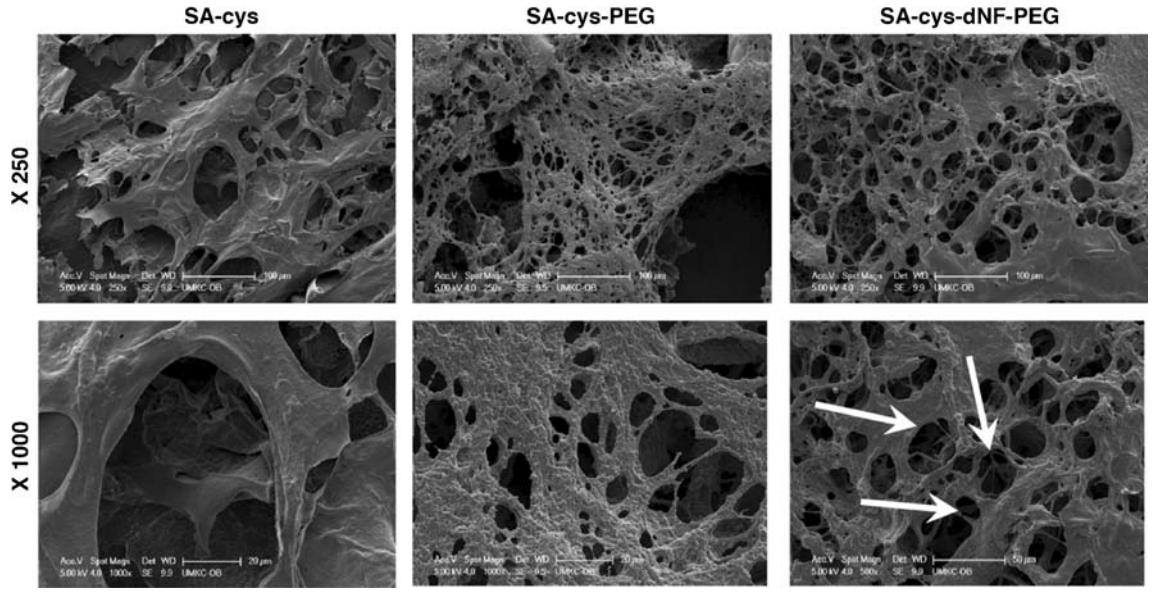

Fig. 5 Morphological characteristics of various hydrogels, such as SA-cys, SA-cys-PEG and SA-cys-dNF-PEG.

rate to those without UV (SA-cys-dNF-PEG: 1.85 ± 0.17 and SA-cys-dNF-PEG with UV: 0.46 ± 0.08 μg/ml/stent, $p < 0.001$), indicating that thiol group reacted with the acrylate group of PEGDA via UV-assisted crosslinking process (i.e. Michael type addition). Given the interaction between thiol and acrylate groups, the reduced thiol contents in the hydrogel scaffolds upon exposure to UV could be responsible for their robust nature and compact architecture structure.

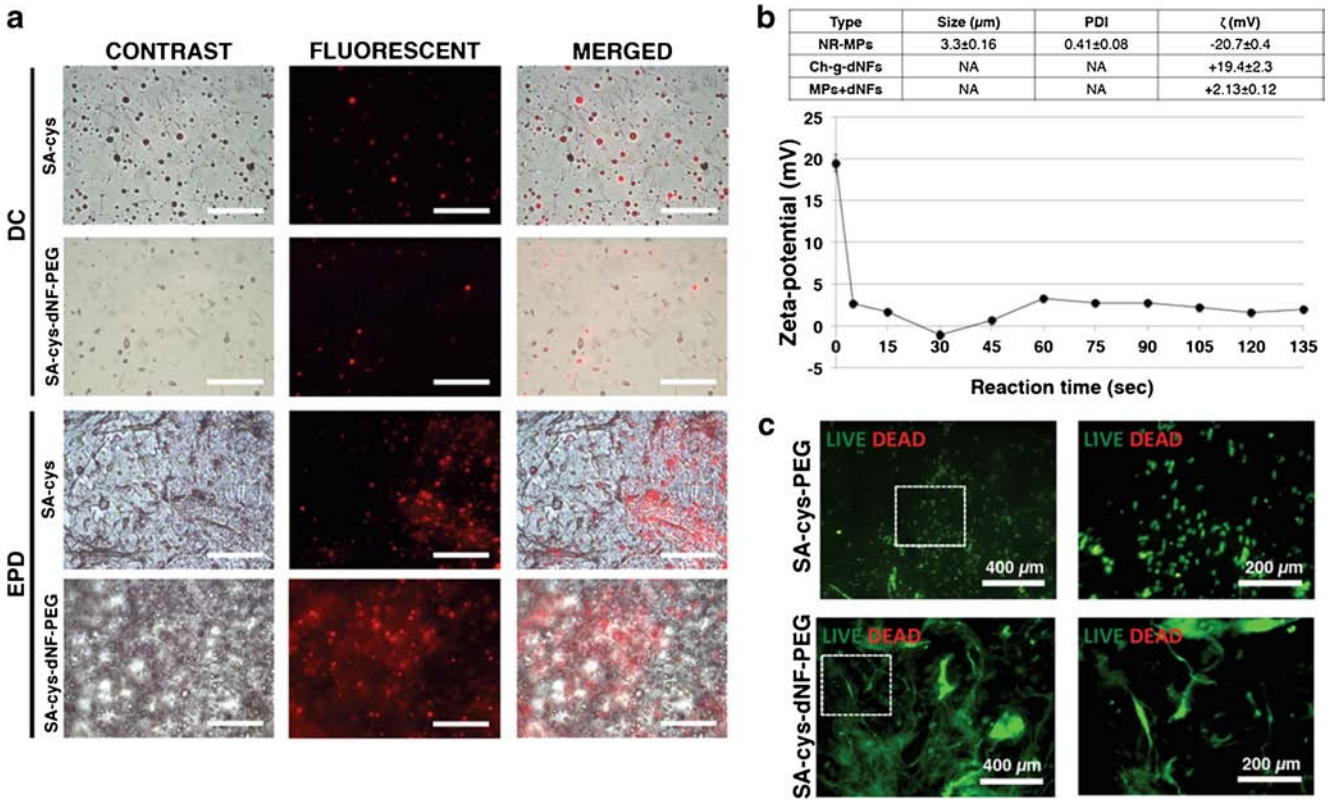

Fig. 6 (**a**) Fluorescent images of NR-MPs distribution in hydrogels with two different coating methods (dip-coating (DC) and eletrophoretic deposition (EPD) technique). (**b**) The size, PDI and zeta-potential of NR-MPs, d-NFs and a mixture of NR-MPs and d-NFs. The changes in zeta-potential of the mixture were recorded during the incubation period ($n = 3$). (**c**) Fluorescent images of AD-MSCs (stained with Live/Dead dyes) encapsulated in hydrogels. The images in the right side are magnified images of *white box* from the images in the left side. The viable cells were visualized in green, whereas dead cells were visualized in read.

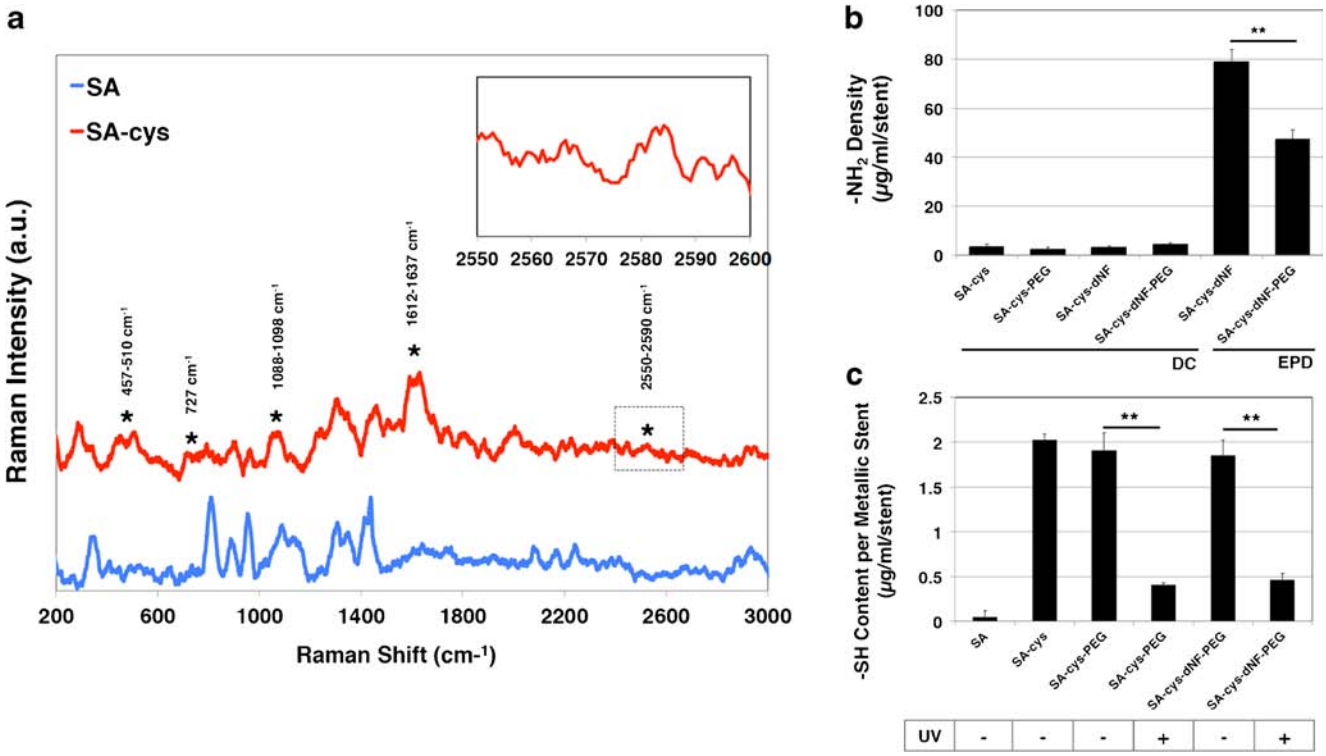

Fig. 7 Raman spectroscopy before and after UV-assisted crosslinking in hydrogels. (**a**) Raman spectroscopy (**b**) Determination of primary amine groups ($-NH_2$) grafted on the surface of d-NFs using Ninhydrin derivatization. (**c**) Determination of thiol ($-SH$) content in metallic stent with or without UV-assisted polymerization. ** in (**b**) and (**c**) indicates statistical significance ($p < 0.01$, $n = 3$).

Evaluation of Swelling Ratio of Various Formulations

The changes in the swelling ratio induced by the components of hydrogel scaffolds were determined by measuring the water uptake content. As shown in Fig. 8, the swelling ratios for SA-cys and SA-cys-dNF after the incubation for 60 min were significantly greater than those for SA-cys-PEG and SA-cys-dNF-PEG (131.2 ± 9.1% for SA-cys, 97.9 ± 10.1% for SA-cys-dNF, 46.1 ± 12.5% for SA-cys-PEG and 35.2 ± 10.9% for SA-cys-dNF-PEG). SA-cys-dNF-PEG prepared using the EPD technique offered the improved mechanical property due to the enhanced swelling ratio as compared to hydrogel scaffolds of SA-cys and SA-cys-dNF.

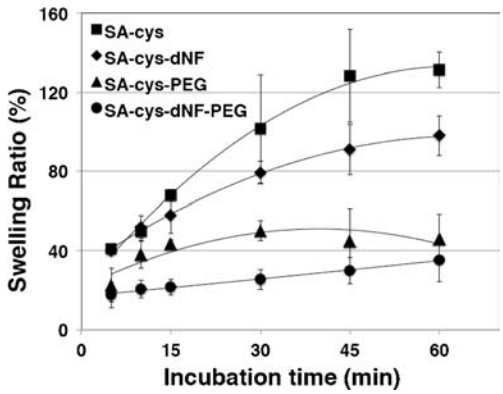

Fig. 8 *in vitro* swelling ratio of hydrogel scaffolds ($n = 3$).

Mechanical Characteristics of Hydrogel Scaffolds

Because the perfused fluid in the vessel created a continuous wall stresses, the mechanical properties against the perfused fluid should be characterized. The custom designed microfluidic simulator under the given settings (i.e. inner radius of tube ($a = 0.75 \times 10^{-3}$ m), viscosity ($\mu = 0.00098$ Pa-s) and flow rate ($Q = 1$ ml/s)) can imitate the physiological dynamic conditions (37°C) including wall stresses (30 dyn/cm^2) (i.e., physiological wall stresses of 2–16 dyn/cm^2). The system could offer an enormous potential to be applicable to *in vitro* assessment of physicodynamic properties of the biomedical devices including cardiovascular stents.

A microfluidic simulator system (Fig. 9a), which is connected to the steady flow chamber and temperature controller, was designed for the assessment of the mechanical strength of the hydrogel-coated stents. The inner surface of tygon tubes was subjected to exposure to the maximum pressure value of 30 dyn/cm^2 (26), which can provide the tested stents with sufficient pseudo-physiological wall stresses of approximately 2–16 dyn/cm^2 (37).

The residence time of NR-MPs encapsulated in the hydrogel scaffolds was evaluated to determine whether or not they

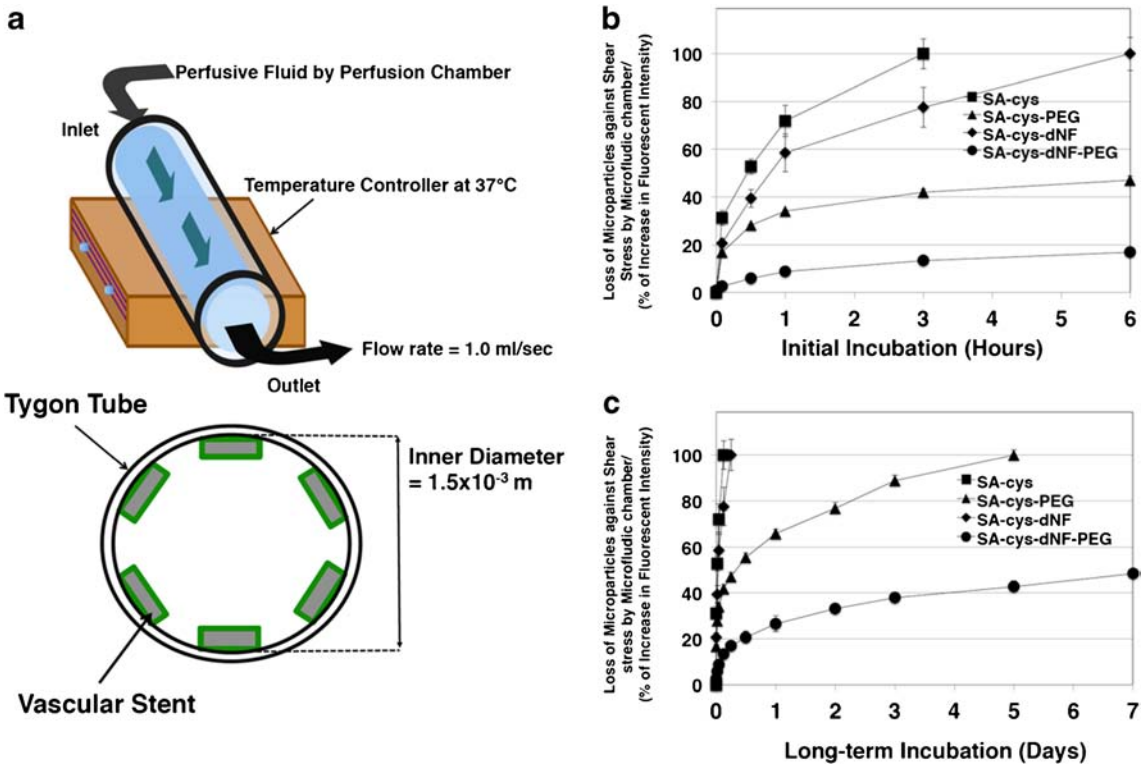

Fig. 9 *in vitro* stability of hydrogel scaffolds against shear stress by continuous flow. (**a**) Description of custom built microfluidic perfusion device with temperature controller. (**b**) and (**c**) Percentage of loss of NR-MPs against shear stress in short-term incubation (**b**) and in long-term incubation (C') ($n = 3$).

are protected from the perfused flow for an extended period of time. Most hydrogels in SA-cys-only were washed out by perfused flow within 3 h, whereas those in SA-cys-dNF lasted for 6 h. As compared to other hydrogels, SA-cys-PEG and SA-cys-dNF-PEG were highly stable (Fig. 9b) and it took a longer period of time for them to be fully washed out by perfused flow (Fig. 9c). SA-cys-PEG was fully disintegrated by perfused flow after incubation for 5 days in a pseudo-microfluidic simulator, whereas only 50% of initial loading amount of SA-cys-dNF-PEG was disintegrated for 7 days. It can be concluded that d-NFs plays a critical role in maintaining mechanical stability of the hydrogel scaffolds under the long-term incubation process and that d-NFs had a mild impact on the mechanical property of SA-cys-dNF. Whereas polymer layers for both SA-cys-PEG and SA-cys-dNF-PEG seemed to be predominantly crosslinked by homopolymerization of PEG-diacrylate (PEGDA). The addition of PEGDA in hydrogel scaffolds during the EPD process has improved the mechanical property against the perfusive fluid through expediting the polymerization process within the time of a short surgical procedure or before the material to be encapsulated disperses.

The mechanical strength of the hydrogel-coated stents against the perfused fluid was evaluated using a pseudo-microfluidic simulator system with the initial moisture maintained throughout the study. The system was placed under the microscope for the assessment of the fluorescent images at different time intervals (i.e. initial, 5 min and 30 min). SA-cys-only group showed a rapid disintegration of coated hydrogel within 5 min, whereas SA-cys-dNF showed a moderate disruption for up to 30 min (Fig. 10). Both SA-cys-PEG and

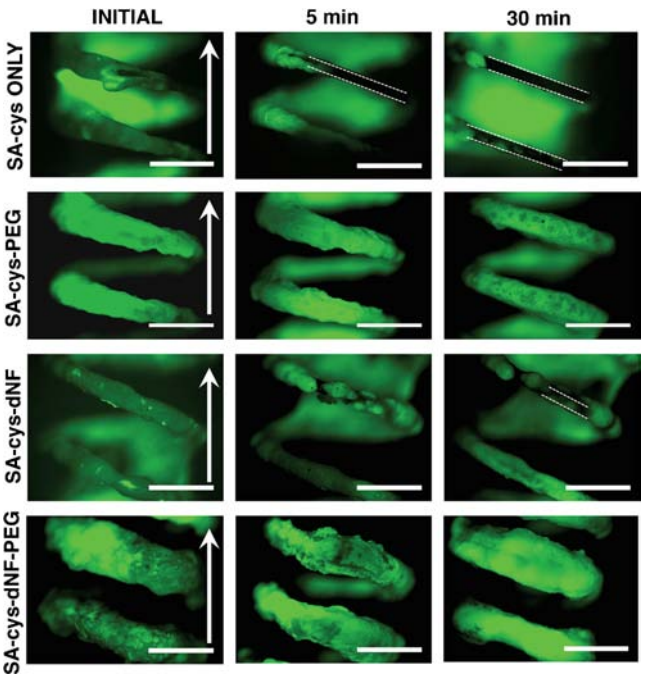

Fig. 10 Fluorescent images of hydrogel scaffolds. *White arrows* indicated the direction of continuous flow. *White dash lines* represented metal surfaces. Scale bar indicated 1 mm.

SA-cys-dNF-PEG showed an enhanced the mechanical property during a 30-min incubation period, confirming the integral role of PEGDA in maintaining the stability of the coated hydrogel. These results were in a close agreement with the previous reports that the acrylate groups formed chemical bonds with amine and thiol groups present in both d-NFs and alginate via Michael-type addition (36). These chemical bonds seem to provide the hydrogel with the robust structure and high stability against the perfused flow.

It is well known that calcium aggravated atherosclerosis, as the elevated level of intracellular calcium triggered endoplasmic reticulum stress (38). Moreover, stem cell niche that has the high concentration of calcium induced osteogenic differentiation of MSCs (39,40), suggesting that metallic surfaces contaminated with calcium may not achieve endothelialization, unless calcium is thoroughly removed. The nanocomposites (d-NFs with SA-cys) developed in this study did not have any divalent cationic ions (i.e. Ca^{++}), and thus can serve as an ideal platform for the enhancement of immunomodulatory efficacy of MSCs.

Assessment of Cytotoxicity of Hydrogel Scaffolds

To examine the biocompatibility of the hydrogel scaffolds, LDH assay was performed on AD-MSCs upon exposure to tested hydrogels of various conditions for 48 h. For the positive control, the cells were lysed with 1% of Triton X-100 and the levels of LDH leakage from lysed cells were determined. No cytotoxicity of AD-MSCs was observed after 48 h exposure to SA-cys at the concentrations of 0–2 mg/ml or d-NFs at the concentrations of 0–0.8 mg/ml (Fig. 11a). In addition, there were no significant differences in cytotoxicity between the groups with or without UV crosslinking (Fig. 11b).

To further determine whether or not the EPD technique used for the hydrogel coating process could exert any cytotoxicities, AD-MSCs stained with fluorescent live/dead dyes (green for live cells and red for dead cells) were assessed using LDH assay. AD-MSCs exposed to the hydrogel coated stents via EPD technique displayed distinctive green signals, indicating that EPD technique exerts no significant cytotoxicity (Fig. 11c).

It was shown that AD-MSCs were densely packed with d-NFs in the hydrogel scaffolds. However, strong spherical green signals were displayed from the cells encapsulated within SA-cys-PEG, indicating that they can offer a suitable cell niche to AD-MSCs (Fig. 11c). It was previously reported that an engineered stem cell niche provided by biomaterials not only enhanced the

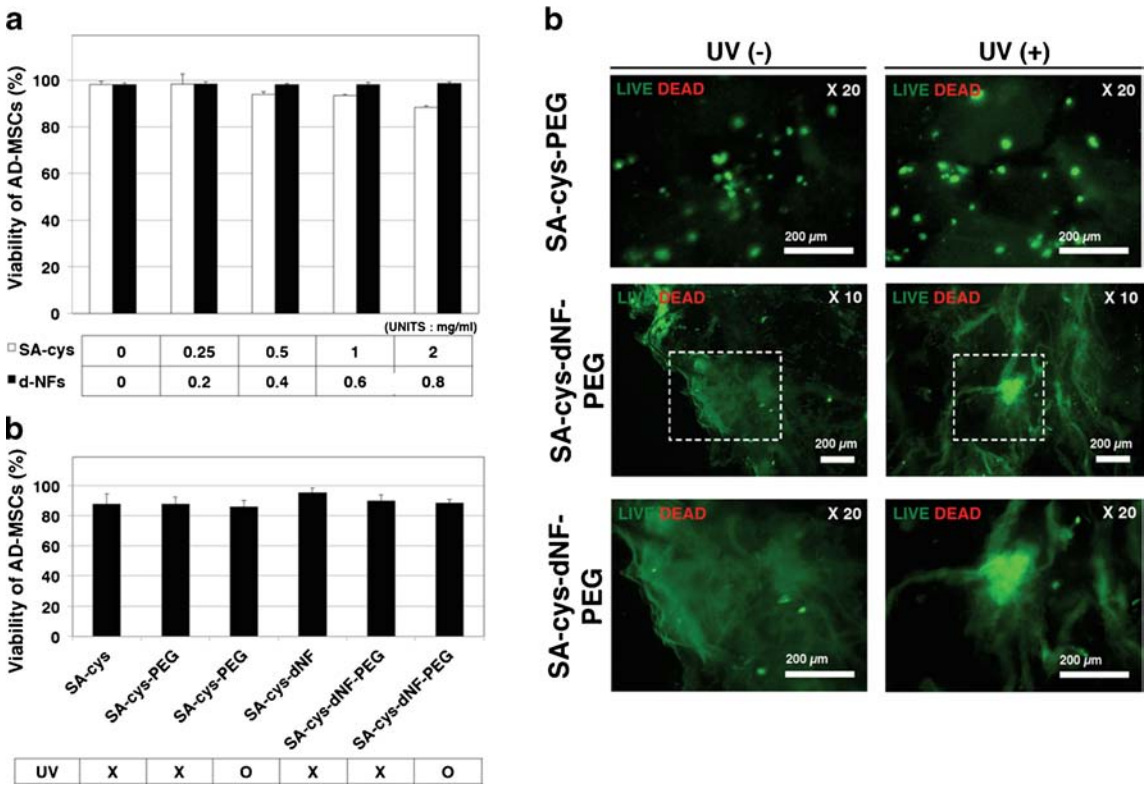

Fig. 11 Cell viability of AD-MSCs. (**a**) Percentage viability of AD-MSCs in presence of SA-cys and d-NFs ($n = 3$). (**b**) Percentage of viability of AD-MSCs encapsulated in hydrogels ($n = 3$). (**c**) Florescent images for Live/Dead assay in the presence and absence of UV-assisted polymerization. Bottom figures indicate florescent images of hydrogel scaffold (SA-cys-dNF-PEG) with high magnification of white boxes presented in middle of figures. All scale bars with size were shown in figures.

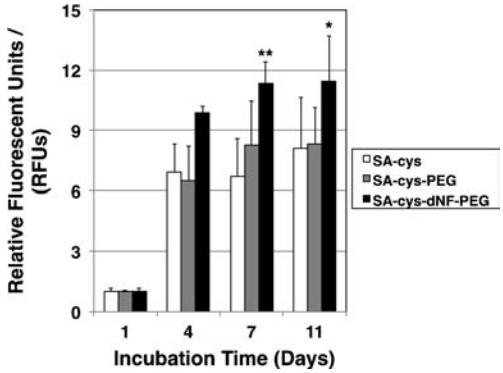

Fig. 12 Proliferation rates of AD-MSCs in TCP, SA-cys, SA-cys-PEG and SA-cys-dNF-PEG. * and ** demonstrate statistical significances of SA-cys-dNF-PEG in comparisons with SA-cys and SA-cys-PEG (* and ** indicate $p < 0.05$ and $p < 0.01$, $n = 3$, respectively).

proliferation rate but also regulated the stem cell lineage (19,41,42).

As the formulations developed in this manuscript are intended for cardiovascular applications, their hemocompatibility also needs to be addressed. A hemocompatibility of hydrogel scaffolds fabricated with sodium alginate, which are physicodynamically similar to the products in this manuscript, was previously reported to be biocompatible and hemocompatible (43–45). The present study supported that the bio-mimetic hydrogels produced by a facile and reproducible fabrication process can be used as a biocompatible platform for recovery of cell mediated endothelialization.

The Proliferation Rates of AD-MSCs in Hydrogel Scaffolds

To evaluate the effects of d-NFs on the proliferation rate of AD-MSCs, the fluorescent intensity of the hydrogels containing AD-MSCs were examined upon being treated with alamar blue reagent (Fig. 12). The fluorescent intensities of the hydrogel scaffolds (SA-cys-dNF-PEG) were significantly greater than those of SA-cys and SA-cys-PEG ($F = 15.724$ and $p < 0.001$ for day 7, and $F = 6.289$ and $p = 0.016$ for day 11), confirming that d-NFs but not PEG enhanced the proliferation rate of AD-MSCs and promoted its stability against the perfused flow. It was previously reported that a spheroid formation of MSCs induced by fragmented nanofibers composites created proper stem cell niche which showed an increase in proliferation rate during the incubation for 2 weeks (19) and was closely correlated with the outcomes from this study.

Effects of ROS on Immunomodulatory Activity of AD-MSCs

To evaluate the immunomodulatory activity of AD-MSCs in the presence or absence of external ROS, the level of L-kynurenine, a tryptophan metabolite, in AD-MSCs was determined as a replacement compound with Indoleamine 2,3-Dioxygenase (IDO). AD-MSCs seeded on tissue-culture plate (TCP) were treated with varying concentrations of ROS (provided by hydrogen peroxide) (Fig. 13a). As the ROS level

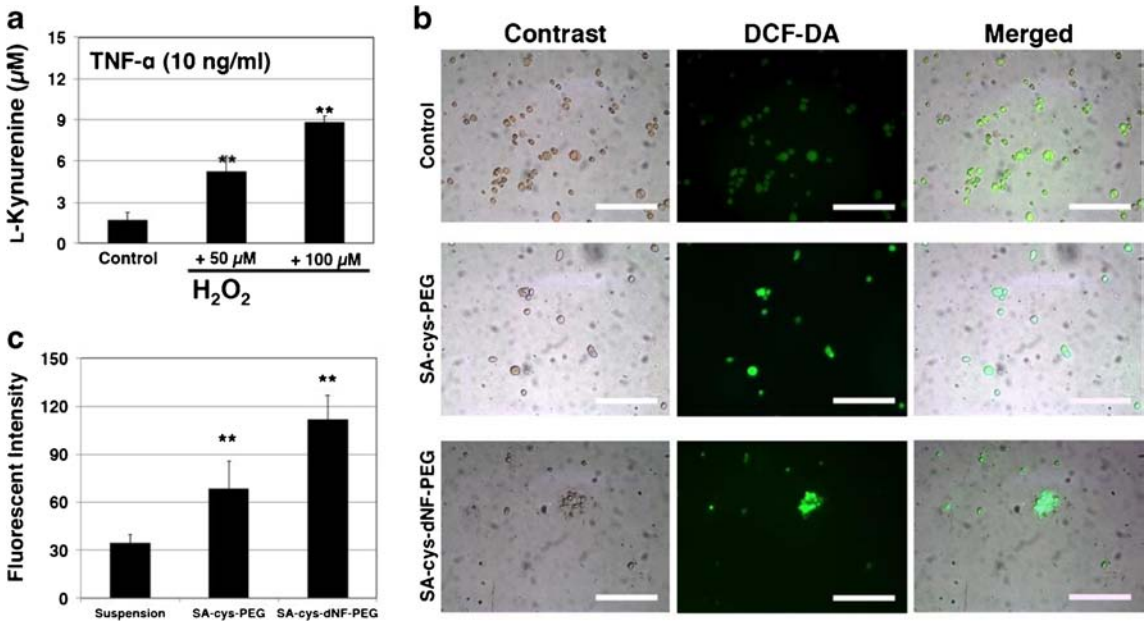

Fig. 13 Immunoregulatory function of AD-MSCs. (**a**) The concentration of L-kynurenine on TCP with ROS treatment. (**b**) Fluorescent images of ROS at subcellular level using ROS sensitive dye (2′,7′ –dichlorofluorescin diacetate, DCFDA). Scale bars indicate 200 μm. (**c**) Measurements of subcellular ROS level determined by green fluorescent signals using ImageJ. ** indicates significant differences between negative, SA-cys-PEG and SA-cys-dNF-PEG ($p < 0.01$, $n = 3$).

increased, the concentration of L-kynurenine increased with a greater rate than those treated with only TNF-α (1.67 ± 0.6 μM without H_2O_2, 5.2 ± 1.14 μM with 50 μM of H_2O_2 and 8.8 ± 0.51 μM with 100 μM of H_2O_2). The results of this study supported that an enhanced subcellular level of ROS by spheroidal cluster yielded IDO-mediated tryptophan replacement.

The generation of ROS were assessed based on the fluorescent intensity reflected from the ROS sensitive dye (2′,7′ – dichlorofluorescin diacetate, DCFDA) (Fig. 13b). A bright green signal was distinctively observed from SA-cys-dNF-PEG, whereas there was a weaker signal from suspension and SA-cys-PEG. In addition, a strong signal was observed from the spheroidal formation of SA-cys-dNF-PEG. The fluorescent intensities of the hydrogel scaffolds encapsulated with AD-MSCs were greater than those of suspended SA-cys-PEG (without AD-MSCs) (34.1 ± 5.8 for suspension, 68.1 ± 17.6 for SA-cys-PEG and 111.7 ± 14.8 for SA-cys-dNF-PEG) (Fig. 13c), indicating that AD-MSCs produced intercellular ROS, even though the produced amount is too low to exert any significant cytotoxic effects.

There has been an increase in awareness of developing an advanced cardiovascular stent to achieve high biocompatibility and therapeutic efficacy without causing any late stage side effects, such as thrombosis and re-stenosis. However, conventional vascular stents including drug-eluting stent (DES) failed to achieve the sufficient endothelialization progress at the surface contact sites. Moreover, no attempt to add any immunoregulatory components to vascular stent has been made. In light of the recent development of stem cell engineering for regenerative medicine, cell therapy utilizing an immunoregulatory function of AD-MSCs against coronary artery disease (CAD) could be an ideal strategy for rapid-endothelialization and stabilization of the immune-responses against the external stimuli (i.e. angioplasty).

Various cell delivery carriers, such as nanofiber sheets, polymeric particles and hydrogels, have been investigated (46–48). Hydrogels are one of the ideal candidates for tissue engineering because their physicochemical characteristics are similar to those of the extracellular matrix (49). The electrophoretical deposition (EPD) technique opened a novel way to coat the metallic surface of cardiovascular stents with the hydrogel scaffolds (18,50,51). Moreover, the robust hydrogel could endure a continuous blood perfusion at the atherosclerotic lesion. The engineered hydrogels (i.e. hydrogels composited with nanofibers) had strong mechanical property and long-term biocompatibility, and thus can serve as an optimal stem cell niche for enhancement of immunoregulatory efficacy.

CONCLUSION

The biomimicking "mud-and-straw bird nest" was developed as a bio-inspired hydrogel-nanofiber carrier for adipose derived human mesenchymal stem cells (AD-MSCs) and evaluated for its potential as the surface coating substrate of drug eluting stent (DES). There were significant effects of the d-NFs and cysteine conjugation on the hydrogel made of sodium alginate. The hydrogels deposited on cardiovascular stent are robust in mechanical property and displayed a huge potential to be applicable to the perfused fluid in the vessel. Moreover, the "mud-and-straw" hydrogel could serve as an ideal niche for attachment and proliferation of AD-MSCs with immune-modulatory properties. The novel stents embedded with biomimicking hydrogels containing AD-MSCs could serve as a promising platform for the efficient treatment strategy against CAD.

ACKNOWLEDGMENTS AND DISCLOSURES

This research was supported in part by funds provided from Graduate Studies Research Grant program, UMKC and Dean's Bridge Fund program from School of Pharmacy, UMKC.

REFERENCES

1. Lusis AJ. Atherosclerosis. Nature. 2000;407:233–41.
2. Maisel WH. Unanswered questions–drug-eluting stents and the risk of late thrombosis. N Engl J Med. 2007;356:981–4.
3. Hulsmans M, Van Dooren E, Holvoet P. Mitochondrial reactive oxygen species and risk of atherosclerosis. Curr Atheroscler Rep. 2012;14:264–76.
4. Oh B, Lee CH. Nanofiber for cardiovascular tissue engineering. Expert Opin Drug Deliv. 2013;10:1565–82.
5. Oh B, Lee CH. Nanofiber-coated drug eluting stent for the stabilization of mast cells. Pharm Res. 2014;31:2463–78.
6. Kode JA, Mukherjee S, Joglekar MV, Hardikar AA. Mesenchymal stem cells: immunobiology and role in immunomodulation and tissue regeneration. Cytotherapy. 2009;11:377–91.
7. Nauta AJ, Fibbe WE. Immunomodulatory properties of mesenchymal stromal cells. Blood. 2007;110:3499–506.
8. Nakajima H, Uchida K, Guerrero AR, Watanabe S, Sugita D, Takeura N, *et al.* Transplantation of mesenchymal stem cells promotes an alternative pathway of macrophage activation and functional recovery after spinal cord injury. J Neurotrauma. 2012;29:1614–25.
9. Jiang XX, Zhang Y, Liu B, Zhang SX, Wu Y, Yu XD, *et al.* Human mesenchymal stem cells inhibit differentiation and function of monocyte-derived dendritic cells. Blood. 2005;105:4120–6.
10. Zanotti L, Sarukhan A, Dander E, Castor M, Cibella J, Soldani C, *et al.* Encapsulated mesenchymal stem cells for in vivo immunomodulation. Leukemia. 2013;27:500–3.
11. Hsu WT, Lin CH, Chiang BL, Jui HY, Wu KK, Lee CM. Prostaglandin E2 potentiates mesenchymal stem cell-induced IL-10+IFN-gamma+CD4+ regulatory T cells to control transplant arteriosclerosis. J Immunol. 2013;190:2372–80.
12. Engela AU, Baan CC, Dor FJ, Weimar W, Hoogduijn MJ. On the interactions between mesenchymal stem cells and regulatory T cells for immunomodulation in transplantation. Front Immunol. 2012;3:126.

13. Chen SL, Zhu CC, Liu YQ, Tang LJ, Yi L, Yu BJ, *et al.* Mesenchymal stem cells genetically modified with the angiopoietin-1 gene enhanced arteriogenesis in a porcine model of chronic myocardial ischaemia. J Int Med Res. 2009;37:68–78.
14. Abdi R, Fiorina P, Adra CN, Atkinson M, Sayegh MH. Immunomodulation by mesenchymal stem cells: a potential therapeutic strategy for type 1 diabetes. Diabetes. 2008;57:1759–67.
15. Yao L, Heuser-Baker J, Herlea-Pana O, Iida R, Wang Q, Zou MH, *et al.* Bone marrow endothelial progenitors augment atherosclerotic plaque regression in a mouse model of plasma lipid lowering. Stem Cells. 2012;30:2720–31.
16. De Miguel MP, Fuentes-Julian S, Blazquez-Martinez A, Pascual CY, Aller MA, Arias J, *et al.* Immunosuppressive properties of mesenchymal stem cells: advances and applications. Curr Mol Med. 2012;12:574–91.
17. Wang J, Lin L, Cheng Q, Jiang L. A strong bio-inspired layered PNIPAM-Clay nanocomposite hydrogel. Angew Chem Int Ed. 2012;51:4676–80.
18. Shi X-W, Tsao C-Y, Yang X, Liu Y, Dykstra P, Rubloff GW, *et al.* Electroaddressing of cell populations by co-deposition with calcium alginate hydrogels. Adv Funct Mater. 2009;19:2074–80.
19. Kim TG, Park S-H, Chung HJ, Yang D-Y, Park TG. Hierarchically assembled mesenchymal stem cell spheroids using biomimicking nanofilaments and microstructured scaffolds for vascularized adipose tissue engineering. Adv Funct Mater. 2010;20:2303–9.
20. Wegst UG, Bai H, Saiz E, Tomsia AP, Ritchie RO. Bioinspired structural materials. Nat Mater. 2015;14:23–36.
21. Jindal AB, Wasnik MN, Nair HA. Synthesis of thiolated alginate and evaluation of mucoadhesiveness, cytotoxicity and release retardant properties. Indian J Pharm Sci. 2010;72:766–74.
22. Yoo JW, Lee JS, Lee CH. Characterization of nitric oxide-releasing microparticles for the mucosal delivery. J Biomed Mater Res A. 2010;92:1233–43.
23. Oh B, Lee CH. Advanced cardiovascular stent coated with nanofiber. Mol Pharm. 2013;10:4432–42.
24. Cui W, Cheng L, Li H, Zhou Y, Zhang Y, Changa J. Preparation of hydrophilic poly(l-lactide) electrospun fibrous scaffolds modified with chitosan for enhanced cell biocompatibility. Polymer. 2012;53:2298–305.
25. Zhong X, Lu Z, Valtchev P, Wei H, Zreiqat H, Dehghani F. Surface modification of poly(propylene carbonate) by aminolysis and layer-by-layer assembly for enhanced cytocompatibility. Colloids Surf B: Biointerfaces. 2012;93:75–84.
26. Shinohara S, Kihara T, Sakai S, Matsusaki M, Akashi M, Taya M, *et al.* Fabrication of in vitro three-dimensional multilayered blood vessel model using human endothelial and smooth muscle cells and high-strength PEG hydrogel. J Biosci Bioeng. 2013;116:231–4.
27. Ankrum JA, Dastidar RG, Ong JF, Levy O, Karp JM. Performance-enhanced mesenchymal stem cells via intracellular delivery of steroids. Sci Rep. 2014;4:4645.
28. Ren G, Su J, Zhang L, Zhao X, Ling W, L'Huillie A, *et al.* Species variation in the mechanisms of mesenchymal stem cell-mediated immunosuppression. Stem Cells. 2009;27:1954–62.
29. Ma S, Xie N, Li W, Yuan B, Shi Y, Wang Y. Immunobiology of mesenchymal stem cells. Cell Death Differ. 2013;21:216–25.
30. Francois M, Romieu-Mourez R, Li M, Galipeau J. Human MSC suppression correlates with cytokine induction of indoleamine 2,3-dioxygenase and bystander M2 macrophage differentiation. Mol Ther. 2012;20:187–95.
31. Braun D, Longman RS, Albert ML. A two-step induction of indoleamine 2,3 dioxygenase (IDO) activity during dendritic-cell maturation. Blood. 2005;106:2375–81.
32. Roemeling-van Rhijn M, Mensah FK, Korevaar SS, Leijs MJ, van Osch GJ, Ijzermans JN, *et al.* Effects of hypoxia on the immunomodulatory properties of adipose tissue-derived mesenchymal stem cells. Front Immunol. 2013;4:203.
33. Liu Y, Wang W, Acharya G, Shim YB, Choi ES, Lee CH. Advanced stent coating for drug delivery and in vivo biocompatibility. J Nanoparticle Res. 2014;15:1–16.
34. McLaughlin SGA, Szabo G, Eisenman G, Ciani SM. Surface charge and the conductance of phospholipid membranes*. Proc Natl Acad Sci U S A. 1970;67:1268–75.
35. Schmid T, Messmer A, Yeo BS, Zhang W, Zenobi R. Towards chemical analysis of nanostructures in biofilms II: tip-enhanced Raman spectroscopy of alginates. Anal Bioanal Chem. 2008;391:1907–16.
36. Read ES, Thompson KL, Armes SP. Synthesis of well-defined primary amine-based homopolymers and block copolymers and their Michael addition reactions with acrylates and acrylamides. Polym Chem. 2010;1:221–30.
37. Cheng C, Helderman F, Tempel D, Segers D, Hierck B, Poelmann R, *et al.* Large variations in absolute wall shear stress levels within one species and between species. Atherosclerosis. 2007;195:225–35.
38. Shrestha S, Irvin MR, Grunfeld C, Arnett DK. HIV, inflammation, and calcium in atherosclerosis. Arterioscler Thromb Vasc Biol. 2014;34:244–50.
39. Liu J, Chen W, Zhao Z, Xu HH. Reprogramming of mesenchymal stem cells derived from iPSCs seeded on biofunctionalized calcium phosphate scaffold for bone engineering. Biomaterials. 2013;34:7862–72.
40. Muller P, Bulnheim U, Diener A, Luthen F, Teller M, Klinkenberg ED, *et al.* Calcium phosphate surfaces promote osteogenic differentiation of mesenchymal stem cells. J Cell Mol Med. 2008;12:281–91.
41. Laschke MW, Schank TE, Scheuer C, Kleer S, Schuler S, Metzger W, *et al.* Three-dimensional spheroids of adipose-derived mesenchymal stem cells are potent initiators of blood vessel formation in porous polyurethane scaffolds. Acta Biomater. 2013;9:6876–84.
42. Huang CC, Chen DY, Wei HJ, Lin KJ, Wu CT, Lee TY, *et al.* Hypoxia-induced therapeutic neovascularization in a mouse model of an ischemic limb using cell aggregates composed of HUVECs and cbMSCs. Biomaterials. 2013;34:9441–50.
43. Notara M, Scotchford CA, Grant DM, Weston N, Roberts GA. Cytocompatibility and hemocompatibility of a novel chitosan-alginate gel system. J Biomed Mater Res A. 2009;89:854–64.
44. Gao W, Lin T, Li T, Yu M, Hu X, Duan D. Sodium alginate/heparin composites on PVC surfaces inhibit the thrombosis and platelet adhesion: applications in cardiac surgery. Int J Clin Exp Med. 2013;6:259–68.
45. Kamouna EA, Kenawyb ES, Tamerc TM, El-Meligyb MA, Eldina MSM. Poly (vinyl alcohol)-alginate physically crosslinked hydrogel membranes for wound dressing applications: characterization and bio-evaluation. Arab J Chem. 2015;8:38–47.
46. Alamein MA, Liu Q, Stephens S, Skabo S, Warnke F, Bourke R, *et al.* Nanospiderwebs: artificial 3D extracellular matrix from nanofibers by novel clinical grade electrospinning for stem cell delivery. Adv Healthcare Mater. 2013;2:702–17.
47. Doshi N, Swiston AJ, Gilbert JB, Alcaraz ML, Cohen RE, Rubner MF, *et al.* Cell-based drug delivery devices using phagocytosis-resistant backpacks. Adv Mater. 2011;23:H105–9.
48. Parisi-Amon A, Mulyasasmita W, Chung C, Heilshorn SC. Protein-engineered injectable hydrogel to improve retention of transplanted adipose-derived stem cells. Adv Healthcare Mater. 2013;2:428–32.
49. Naito H, Yoshimura M, Mizuno T, Takasawa S, Tojo T, Taniguchi S. The advantages of three-dimensional culture in a collagen hydrogel for stem cell differentiation. J Biomed Mater Res A. 2013;101:2838–45.

50. Cheng Y, Tsao C-Y, Wu H-C, Luo X, Terrell JL, Betz J, *et al*. Electroaddressing functionalized polysaccharides as model biofilms for interrogating cell signaling. Adv Funct Mater. 2012;22:519–28.

51. Yang X, Kim E, Liu Y, Shi X-W, Rubloff GW, Ghodssi R, *et al*. In-film bioprocessing and immunoanalysis with electroaddressable stimuli-responsive polysaccharides. Adv Funct Mater. 2010;20: 1645–52.